energies

MDPI

Article

Sintering and Fusibility Risks of Pellet Ash from Different Sources at Different Combustion Temperatures

Juan Carlos Contreras-Trejo [1], Daniel José Vega-Nieva [2], Maginot Ngangyo Heya [3], José Angel Prieto-Ruíz [2], Cynthya Adriana Nava-Berúmen [4] and Artemio Carrillo-Parra [5,*]

1 Maestría Institucional en Ciencias Agropecuarias y Forestales (MICAF), Universidad Juárez del Estado de Durango (UJED), Durango 34100, Mexico; jcarlosct1994@hotmail.com
2 Facultad de Ciencias Forestales y Ambientales, Universidad Juárez del Estado de Durango (UJED), Durango 34120, Mexico; danieljvn@gmail.com (D.J.V.-N.); jprieto@ujed.mx (J.A.P.-R.)
3 Facultad de Agronomía (FA), Universidad Autónoma de Nuevo León (UANL), Escobedo 66050, Mexico; nheyamaginot@yahoo.fr
4 Tecnológico Nacional of México (TecNM), Campus Technological Institute of Valle del Guadiana (ITVG), Villa Montemorelos 34371, Mexico; cynthia1905@yahoo.com.mx
5 Instituto de Silvicultura e Industria de la Madera (ISIMA), Universidad Juárez del Estado de Durango (UJED), Durango 34120, Mexico
* Correspondence: acarrilloparra@ujed.mx

Abstract: Pellets are solid biofuels with a combustion efficiency of 85–90%, low CO_2 emissions and costs, great comfort and versatility. However, the ash generated during combustion can present sintering and fusibility, decreasing boiler efficiency and potentially malfunctioning. Ash composition indexes can be useful to predict observed ash sintering and fusion but require further analysis for a variety of feedstocks. The objective of this work was to determine the effect of the mineral composition of pellet ash from 15 biomasses of forest and agro-industrial sources on observed pellet ash slagging using a laboratory test. The chemical composition of pellets and the indexes B, NaK/B, SiP/CaMg and SiPNaK/CaMg at 550 and 1000 °C were determined. Pearson correlation tests were also performed between cumulative percentages of slag at different sieve sizes. The concentrations of CaO ranged from 4.49 to 65.95%, MgO varied from 1.99 to 17.61%, and the SiO_2 concentration was between 16.11 and 28.24% and 2.19–56.75% at 550 and 1000 °C, respectively. Pellets of forest origin presented a low risk of slag formation, while those from agro-industrial sources showed a high risk of slag formation. The index SiPNaK/CaMg showed the highest correlation ($R^2 > 0.75$) to observed slagging using the BioSlag test.

Keywords: ash; biomass; pellets; slag; sintering

Citation: Contreras-Trejo, J.C.; Vega-Nieva, D.J.; Heya, M.N.; Prieto-Ruíz, J.A.; Nava-Berúmen, C.A.; Carrillo-Parra, A. Sintering and Fusibility Risks of Pellet Ash from Different Sources at Different Combustion Temperatures. *Energies* **2022**, *15*, 5026. https://doi.org/10.3390/en15145026

Academic Editor: Fernando Rubiera González

Received: 24 May 2022
Accepted: 1 July 2022
Published: 9 July 2022

1. Introduction

Pellets are solid biofuels made from biomass densification and are mainly focused on generating energy in the form of heat. Pellet-based heating systems have a combustion efficiency of 85–90%, operate automatically using forced air, generate low CO_2 emissions and have low costs, great comfort and versatility [1–3]. However, despite the benefits of using pellets and biomass for energy purposes, ash sintering and fusibility can limit boiler efficiency and even result in equipment malfunction [4].

The amount of ash produced during the combustion of biomass materials is highly variable, ranging from <1% for some species of conifers, reaching up to 15% in some herbaceous materials and 25% in other agricultural residues [5–7]. The analysis of the feasibility of using pellets from various biomass sources has been mainly based on physical, mechanical and energy properties [8–10]. However, there are relatively fewer works that have analyzed the formation of slags and the processes of sintering of the elements contained in the ash, particularly for pellets from less studied feedstocks. However, these are

some of the most important limitations for using pellets as an energy source in combustion systems [11,12].

The practical problems associated with the ash behavior are sometimes catastrophic and spectacular, ranging from major slag falls that damage the bottoms of furnaces to complete plugging of convection passes. Ash deposits directly affect the internal functioning of the boiler and can affect the design, lifetime and operation of combustion equipment, increase the operating cost, decrease boiler efficiency, deteriorate combustion behavior with higher combustion temperatures, retard heat transfer, cause high temperature corrosion and provoke mechanical failures, which in some cases are irreparable [13,14].

Ash mainly consists of potassium, calcium, sodium, silicon, phosphorus, iron, magnesium and sometimes chlorine and sulfur [15]. Woody biomass has generally low levels of Si and K but is high in Ca [16], whereas agricultural residues are generally high in Si and K but low in Ca. Nevertheless, the chemical constitution of biomass is very heterogeneous, with large variations between species, plant fractions, age, or collection date [17]. While the majority of analyses of ash composition have focused on temperate to boreal tree and herbaceous species [17], there are relatively fewer studies analyzing the ash composition of forest and agricultural feedstocks in semiarid ecosystems and their implications for combustion behavior.

The formation of slags is associated with high concentrations of K and Na that decrease the melting point of the ashes, while the opposite effect is produced by high concentrations of Ca and Mg since they increase the melting point [18,19]. For non-volatile mineral elements such as Si, oxides are formed in the combustion process and adhere to the surface of combustion particles in the form of a molten state [16]. The above affects the combustion process by a series of physical and chemical transformations resulting from the processes of segregation, vaporization, precipitation, nucleation and coalescence [20]. In this way, high concentrations of alkali metals present in the biomass can form potassium silicates, which leads to the formation of slags that can cause sintering, melting and stickiness of the ashes and which favors the corrosion and erosion of combustion boilers [21,22]. The ratio of alkaline earth oxides to alkaline oxides and their representation in a $SiO_2/CaO/K_2O$ ternary phase diagram, based on the analysis of micronutrients from biomass ash, have been used to predict ash behavior [23]. In addition to the above, other indexes have been proposed for the prediction of slag formation, such as the index (B), NaK/B, SiP/CaMg and SiPNaK/CaMg [24,25]. Nevertheless, ash slagging indexes continue to be the subject of ongoing research [26] and still need to be tested over a large variety of biomass sources against observed ash slagging.

Laboratory tests to measure the risk of slag formation include the ash fusibility based on DIN standards [27], the measurement of the compressive strength of previously heated pellet ash, or the manual disintegration of preheated ash [11,16]. The most widely used laboratory test for evaluating ash sintering, the ash fusibility test, has been subject to criticism in the literature (e.g., [28]), frequently predicting a less problematic behavior of various biomass fuels in comparison to the actual slagging tendencies observed in commercial pellet boiler equipment (e.g., [28]). Other methods have also shown limitations: for example, Fernández et al. [11] concluded that the compressive strength was not suitable for predicting ash sintering trends in wood fuels and other biomass with low alkali oxide content, while the manual disintegration test relies on subjective evaluation. Some other methods rely on expensive experimental equipment such as the slag analyzer developed by Hansen and Jensen [29].

The recent *BioSlag* method [25], also named "Testing of Pellet Ash and Slag Sieving Assessing" (PASSA) by Rathbauer et al. [30], is a new and highly recognized method [23,25], developed by the European "AshMelt" research project [30,31] based on the study of Vega-Nieva et al. [25]. The method uses commonly available laboratory equipment and has been validated for the woody and herbaceous biomass fuels of northern [31,32] and southern Europe [4,33]. However, its performance has not yet been evaluated for other fuel sources

of potential economic relevance outside of Europe, the thermal behavior of which in terms of slagging risk remains largely unknown.

In this sense, although the research carried out by Carrillo et al. [10,34] established the possibility of using pellets from different biomass sources in Mexico considering only the physical, mechanical and energy properties, its risk of slagging is still mainly unknown, preventing large-scale use in domestic boilers. Therefore, the objectives of this work were (1) to measure the formation of ash slagging, using the bioslag method, in the combustion of 15 biomass sources from forestry, agricultural and agro-industrial origin which have already been recommended for the production of energy in the form of pellets and (2) to investigate the relationship of observed slag formation with their ash chemical composition and ash slagging indexes at 550 °C as well as to determine the chemical composition of ash and slag at 1000 °C.

2. Materials and Methods

2.1. Biofuel Raw Material Selection and Chemical Characterization

Pellet raw materials were selected from 15 biomass sources of forestry, agricultural, and agro-industrial origin. Table 1 shows the codes for biomass, source, description, as well as the values of their proximate analysis. The pellets selected to determine the level of ash slag were those that in different investigations were recommended for energy generation through physical, mechanical and energy tests [10,34]. They were prepared following the procedure described by Núñez-Retana et al. [34]. The pellets from each source were incinerated in muffle model 1400 FB1415M at 550 °C according to UNE-EN 14775 (2010) [35] and at 1000 °C for the BioSlag test. The concentrations of Al, Ca, Fe, K, Mg, Mn, Na, P and Si of pellet ash samples from each source obtained at 550 °C and 1000 °C were determined through an inductively coupled optical plasma emission spectrophotometer (ICP-OES) [36].

Table 1. Description of 15 different pellet base materials and their proximate analysis.

Code	Species	Source	Biomass Description	Proximate Analysis (%)			
				Moisture Content	Volatile Material	Ash	Fixed Carbon
Pipa	*Pinus patula*	Forest	Pine firewood	6.52	83.90	0.47	15.62
Pidu	*Pinus durangensis*	Forest	Pine firewood	5.79	85.22	0.39	14.39
Quela	*Quercus laeta*	Forest	Oak firewood	5.04	81.28	1.35	17.37
Quesi	*Quercus sideroxyla*	Forest	Oak firewood	4.56	83.06	0.95	15.99
Queco	*Quercus conzattii*	Forest	Oak firewood	4.77	83.71	0.80	15.49
Jun	*Juniperus* sp.	Forest	Tascate firewood	4.96	78.01	0.45	21.54
Pro	*Prosopis* sp.	Forest	Mezquite firewood	6.38	74.55	1.33	17.33
Madol	*Malus domestica*	Agriculture	Apple tree firewood	5.58	82.74	2.12	15.14
Manil	*Mangifera indica*	Agriculture	Mango tree firewood	5.97	80.09	2.63	17.27
Mador	*Malus domestica*	Agriculture	Apple pruns	5.14	80.41	2.46	16.46
Penn	*Pennisetum* sp.	Agriculture	Maralfalfa stubble	5.84	71.93	9.71	18.36
Agat	*Agave tequilana*	Agro-industrial	Agave bagasse	6.60	79.58	10.55	9.87
Cari	*Carya illinoinensis*	Agro-industrial	Walnut peel	5.71	76.01	2.47	21.52
Agad	*Agave durangensis*	Agro-industrial	Agave bagasse	5.84	74.89	12.30	14.48
Manih	*Mangifera indica*	Agro-industrial	Mango bone	6.44	79.02	3.67	17.31

2.2. Slag Prediction Indexes for Pellets from Different Sources at Two Combustion Temperatures

The formation of slag and fouling of the ashes generated at 550 and 1000 °C from the 15 pellet sources was determined through four indexes, as presented in Table 2.

Table 2. Slag indexes based on ash chemical composition at 550 °C and 1000 °C.

Slag Indexes	Description	Source
NaK/B	$(Na_2O + K_2O)/(CaO + MgO + Na_2O + K_2O)$	[25]
B	$CaO + MgO + Fe_2O_3 + Na_2O + K_2O$	[24]
SiP/CaMg	$(SiO_2 + P_2O_5)/(CaO + MgO)$	[25]
SiPNaK/CaMg	$(SiO_2 + P_2O_5 + Na_2O + K_2O)/(CaO + MgO)$	[25]

The NaK/B index relates the content of alkali metals (NaO and KO), elements with high possibilities of slag formation, with earthy alkali metals, elements with a high melting point, which reduces the risk of slag formation. Values higher than 0.50 in this index for a specific type of biomass have been found to result in a high risk of slag formation. On the other hand, index B, called base index or percentage of bases, relates basic elements with acidic elements present in the ashes, and biomasses with low values calculated with this index show a high possibility of slag formation. Additionally, the SiP/CaMg and SiPNaK/CaMg indexes are based on the empirical relationships of ash chemistry, which usually relate the most important elements in the processes of slag formation, agglomeration, and ash fusibility (Si, P, K, Na) with the elements that reduce this risk (Ca, Mg). Biomasses with values higher than 0.5 have been found to present a higher risk of slag formation.

2.3. Slag Formation Test

The BioSlag (Test BioSlag) is a qualitative and quantitative method based on the granulometric determination of the ashes which has shown a good potential to reproduce the slagging observed in combustion process [25,31]. It consisted of placing 250 g of pellets from each of the 15 biomass sources in porcelain crucibles of 284 cm^2 and 5 cm height, with three repetitions. The crucible with the pellet sample was placed in a muffle and the temperature was raised at a rate of 10 °C min^{-1} to reach a temperature of 250 °C, remained constant for 5 h to remove the volatile fraction from the samples. Then the temperature was raised again with the same heating ramp to reach 1000 °C; this final temperature remained constant for 6 h, and at the end the muffle was turned off and after the muffle was cooled down, the crucible was weighed with the burned sample, following the protocol proposed by Vega-Nieva et al. and Schönet et al. [25,31]. Figure 1 shows the ash produced by each biomass source.

The slag and residues were carefully removed from the crucibles for screening by an analytical sieve at 300 rpm for 3 min. Wire meshes with nominal openings of 3.35, 2.00, 0.85, 0.42 and 0.25 mm were used. The weight retained in each sieve was measured and the level of sintering of each sample was measured by manual disintegration, according to the scale shown in Table 3.

2.3.1. Percentage of Calcined Sample of Ash

The percentage of calcined sample was determined from the ash produced from pellets calcined at 1000 °C, according to the following equation:

$$\text{Calcined sample } (\%) = \frac{\text{Mass of calcined sample } (g)}{\text{Mass of pellets sample } (g)} \times 100 \quad (1)$$

2.3.2. Slag Severity Index of Ash

This index is based on the results of the BioSlag test and uses the data of calcined sample (%), level of sintering and granulometric accumulation in the sieves (%). The criteria were scaled from 0 to 1, according to Table 4.

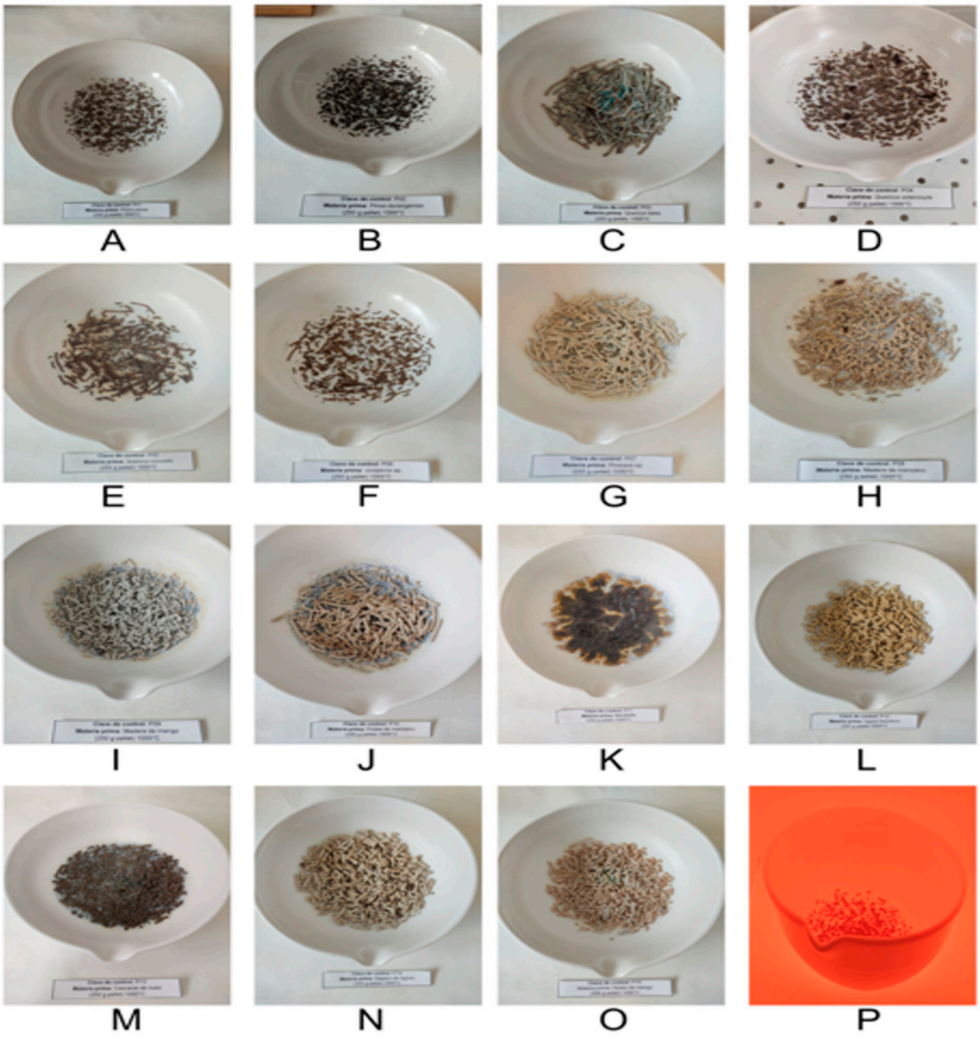

Figure 1. Sintered ash and slag formation from 15 pellet sources subjected to calcination at 1000 °C using the BioSlag test: horizontally (**A**–**G**) pellets from forest sources; (**H**–**K**) pellets from agricultural sources; (**L**–**O**) pellets from agro-industrial sources; (**P**) sintering process at 1000 °C.

Table 3. Level of sintering of biofuels using the BioSlag Test.

Sintering Level	Description
Dust	Non-agglomerated ash
Weak sintering	Agglomerated ash disintegrates under gentle pressure
Hard sintering	Agglomerated ash disintegrates when applying strong pressure
Molten	Ash is completely melted to the crucible

Table 4. Slag severity calculation based on the BioSlag Test.

Class	Calculation
Calcinated percentage index	The percentage values of the calcined samples are divided by the maximum value of 10%.
Sintering level index	The values are classified on dust 0.25, weak sintering 0.5, hard sintering 0.75 and molten 1.
Accumulated slag index	The percentage of accumulated slag on sieves of 3.35, 2 and 0.85 mm is divided by the value of 100.

2.4. Statistical Analysis

The mean values and standard deviations were calculated for the chemical element compositions of the pellet ash from each source, and the compliance with the normality of the data was determined by means of a Shapiro test. The non-parametric Kruskal–Wallis test was used to determine the differences between groups ($p \leq 0.05$). Principal component analysis (PCA) of elemental composition was also applied to reduce the number of primary variables and replace them with components that explain the correlation between the estimated variables and the common information they share, the PCA allows simplification of the interpretation of the results with the maximum amount of information.

Pearson correlation tests were performed between cumulative percentages of slag at different sieve sizes and silica-based indexes SiP/CaMg and SiPNaK/CaMg at temperatures of 550 and 1000 °C.

3. Results

3.1. Chemical Elements Composition of the Pellet Ash from Different Sources

The chemical composition of pellet ash from 15 biomass sources generated at temperatures of 550 and 1000 °C is shown in Figures 2 and 3, and Annexes S1 and S2, respectively. The concentrations of CaO ranged from 8.93 to 65.95% at temperature of 550 °C, while at 1000 °C it was 4.49–61.68%. The content of MgO varied from 3.89 to 13.66 and 1.99 to 17.61%, respectively. The concentrations of alkali metals was as follows: K_2O, 2.18–56.10 and 1.04–27.36%, respectively, and Na_2O, 0.81–2.46 and 1.69–4.12%, respectively. On the other hand, the concentrations of SiO_2 remained between 16.11–28.24 and 2.19–56.75%, respectively. The transition metals were as follows: Fe_2O_3, 0.09–5.12 and 0.27–4.74%, respectively, and MnO between 0.02–3.32 and 0.01–4.49%, respectively. Finally, the concentrations of Al_2O_3 ranged between 0.03–3.69 and 0.26–10.75%, respectively. The concentration of P_2O_5 was 0.55–3.71 and 1.50–19.94% at temperatures of 550 and 1000 °C, respectively.

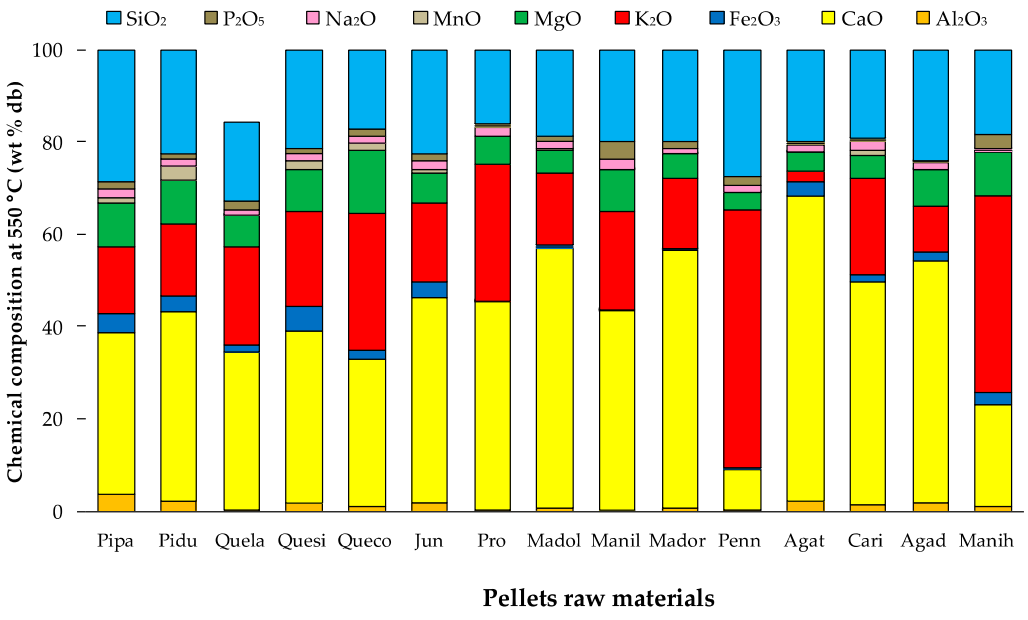

Figure 2. Chemical composition (wt % db) of majority elements of pellet ash from 15 sources calcined at 550 °C.

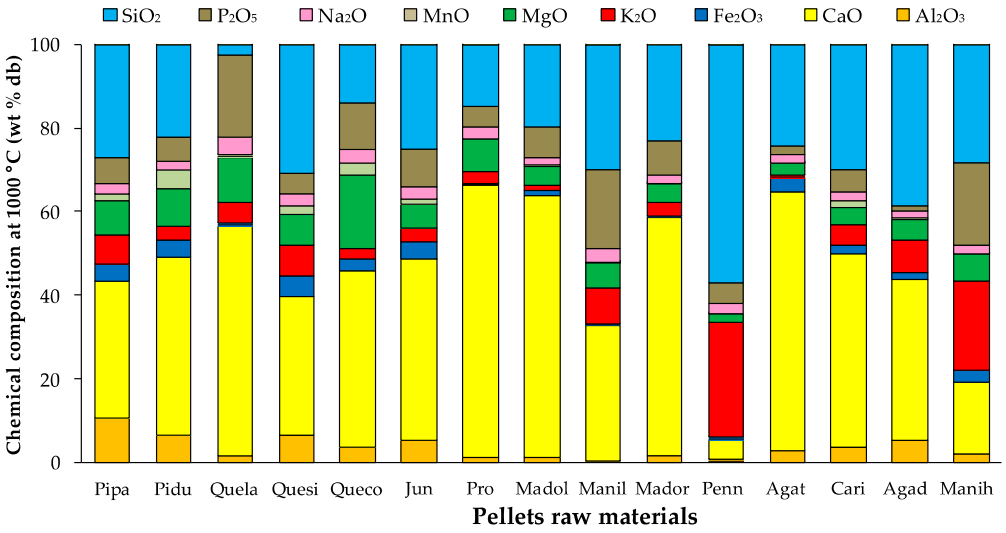

Figure 3. Chemical composition (wt % db) of majority elements of pellet ash from 15 sources subjected to calcination at 1000 °C.

Figures 4 and 5 show the relationships between the concentrations of elements and the pellet sources evaluated by principal component analysis at 550 °C and 1000 °C, respectively. The PCA at 550 °C shows a negative correlation in PC1 and PC2 between the elements P_2O_5 and K_2O for Penn, Manih and Queco pellets. It can be observed that concentrations of MgO, MnO, SiO_2, Fe_2O_3, and Al_2O_3 were positively correlated with PC1 and negatively with PC2. In addition, the concentration of these elements presents similar trend for Pipa, Pidu and Quesi pellets. The concentration of CaO and Na_2O were positively correlated with PC1 and PC2 for Agad, Agat and Cari pellets. Finally, it can be observed that Manil, Madol, Mador and Pro pellets were negatively correlated with PC1 and positively with PC2. It was observed that the concentrations of the elements P_2O5 and K_2O, MnO and SiO_2 and CaO and Na_2O have a high correlation value, while CaO and Fe_2O_3, SiO_2 and P_2O_5 were not correlated.

The PCA at 1000 °C shows that concentrations of P_2O_5, Na_2O, CaO and MgO had a positive correlation with PC1 and negative correlation with PC2 and their concentration affects Madol, Pro, Quela and Queco pellets. It was observed that Al_2O_3, F_2O_3 and MnO had a positive correlation with PC1 and PC2 and mostly affected Pipa, Pidu, Quesi and Jun pellets. The K_2O and SiO_2 elements were negatively correlated with PC1 and positively with PC2 and were related to Penn, Agad and Cari pellets. Finally, Manih, Mador and Mani pellets were negatively correlated with PC1 and PC2.

3.2. Slag Prediction Indexes of Ash from 15 Sources of Pelletized Biomass

Figure 6 and Annex S3 present the four indexes of the prediction slag formation of ash from 15 sources of pelletized biomass calcined at 550 and 1000 °C. Except for the B index at 1000 °C, all calculated indexes showed a non-normal distribution ($p < 0.05$). The Kruskal–Wallis test and the Tukey test showed significant statistical differences ($p \leq 0.05$) between all biomass sources for all slag indexes.

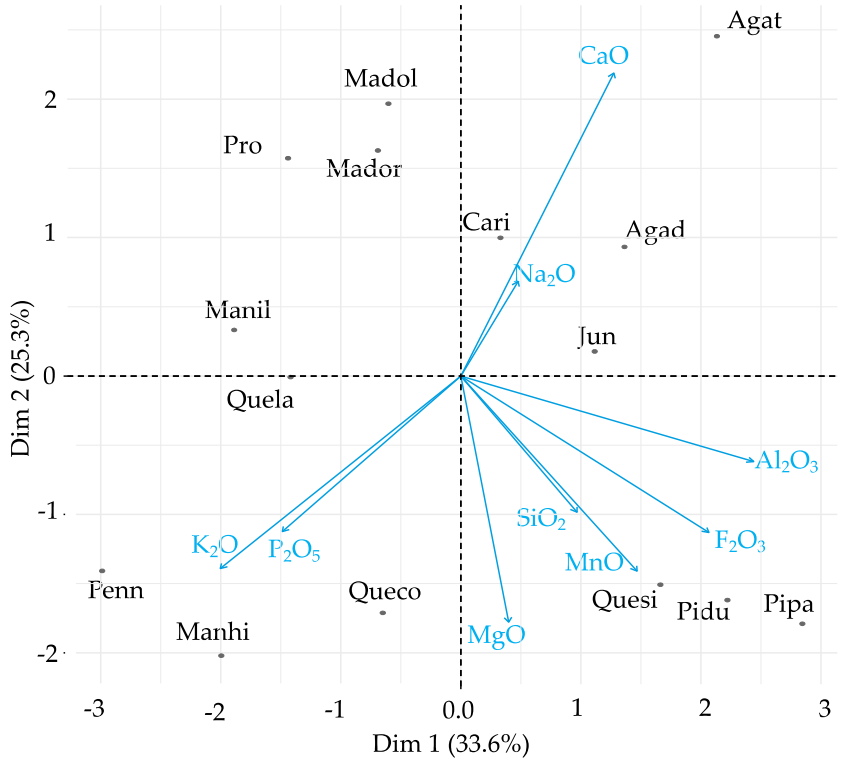

Figure 4. Principal component analysis at 550 °C. Blue lines show the vectors in the CP1 and CP2; the points represent the pellets sources evaluated.

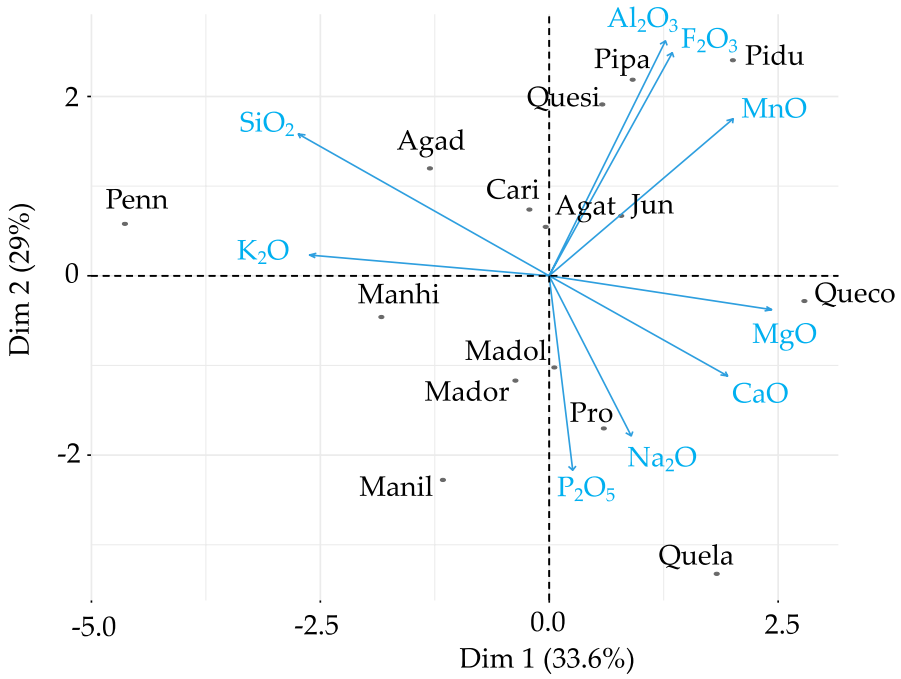

Figure 5. Principal components analysis at 1000 °C. Blue lines show the vectors in the CP1 and CP2, the points represent the pellets sources evaluated.

Most of the pellet ashes tested presented a low risk of slag formation at both temperatures except for Penn and Manih ashes, which showed a high risk of slag formation when using the NaK/B index (>0.5). Similar results for ashes of all origins were found using the SiP/CaMg and SiPNaK/CaMg silica-based indexes. In this work it was found that the B index could not clearly predict the process of slag formation in the evaluated pellets.

The BioSlag test corroborated the high risk of fusibility of Penn pellet ash since the ash was completely melted into the crucible when it was calcined at 1000 °C. The Madol, Manil, Mador and Manih pellets presented a high slag formation in the sieve of 2.0 mm. On the other hand, Agad, Agat, Manih and Mador pellets showed high percentages of slag in the sieve of 3.35 (Figure 7, Annex S4).

The silica-based indexes SiPNaK/CaMg and SiP/CaMg were positively correlated with the results of the BioSlag test when using the sieve >2.00 mm (Figure 8). The highest correlation was observed for the SiPNaK/CaMg index, with $R^2 = 0.75$ (p-value = 2.2×10^{-16}) at 550 °C and $R^2 = 0.77$ (p-value = 6.94×10^{-15}) at 1000 °C, followed by SiP/CaMg, with $R^2 = 0.68$ (p-value = 6.25×10^{-12}) and $R^2 = 0.76$ (p-value = 9.61×10^{-15}) at 550 °C and 1000 °C, respectively (Figure 8).

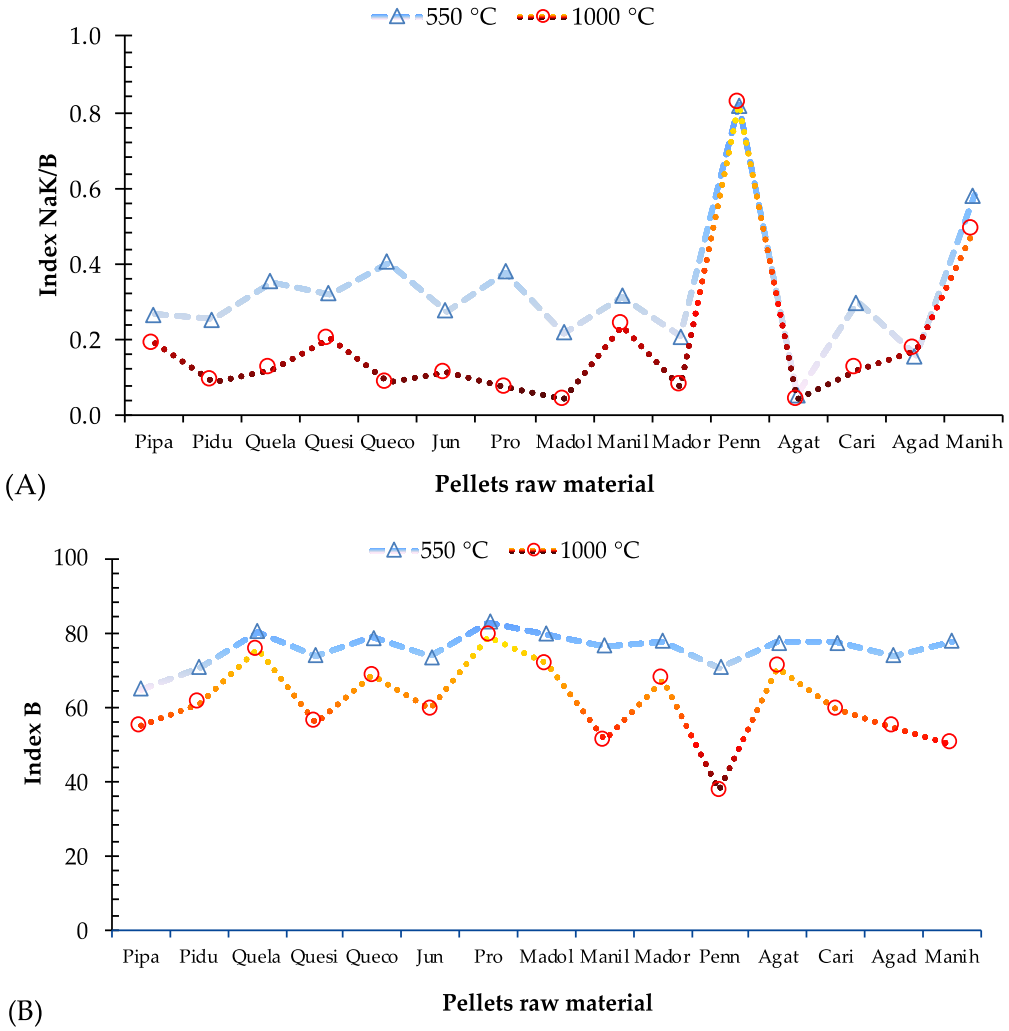

Figure 6. *Cont.*

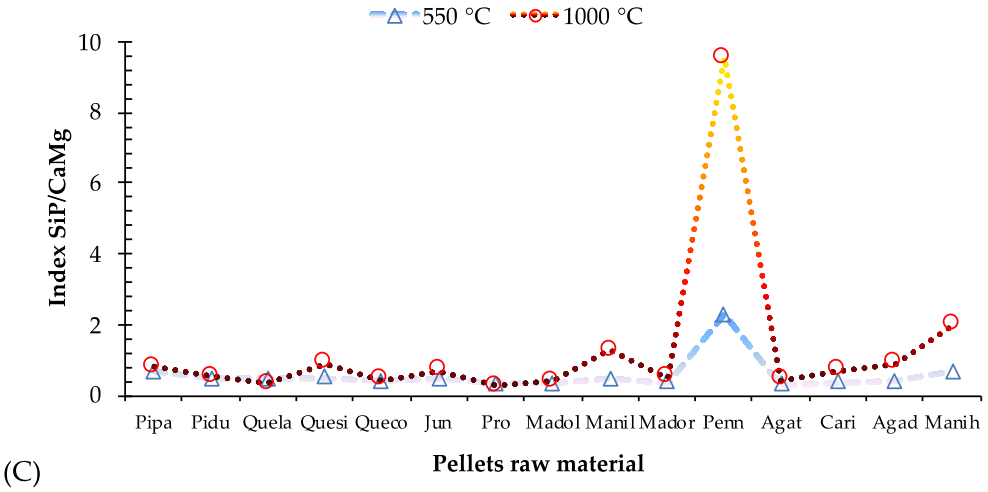

(C)

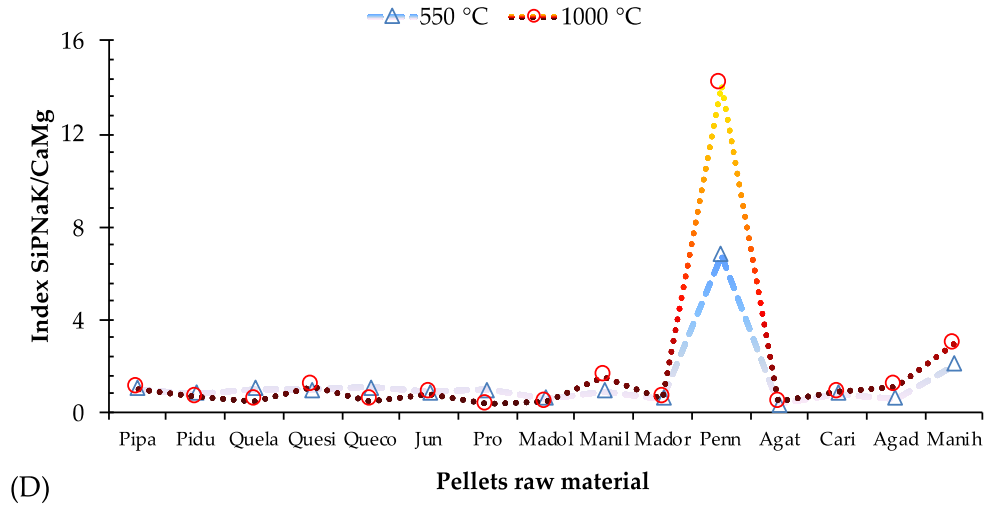

(D)

Figure 6. Slag indexes from 15 pelletized biomass sources calcined at 550 °C and 1000 °C temperatures. (**A**) Index NaK/B, (**B**) Index B, (**C**) Index SiP/CaMg and (**D**) SiPNaK/CaMg.

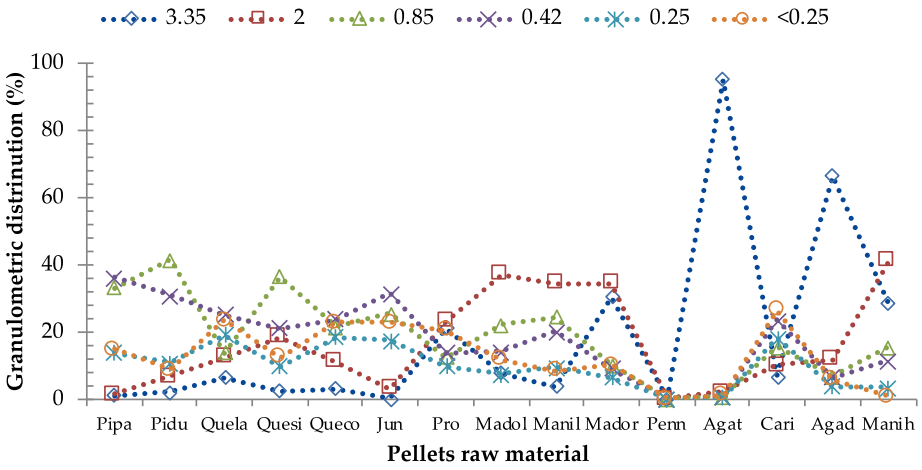

Figure 7. Granulometric distribution of ash from 15 pelletized biomass sources.

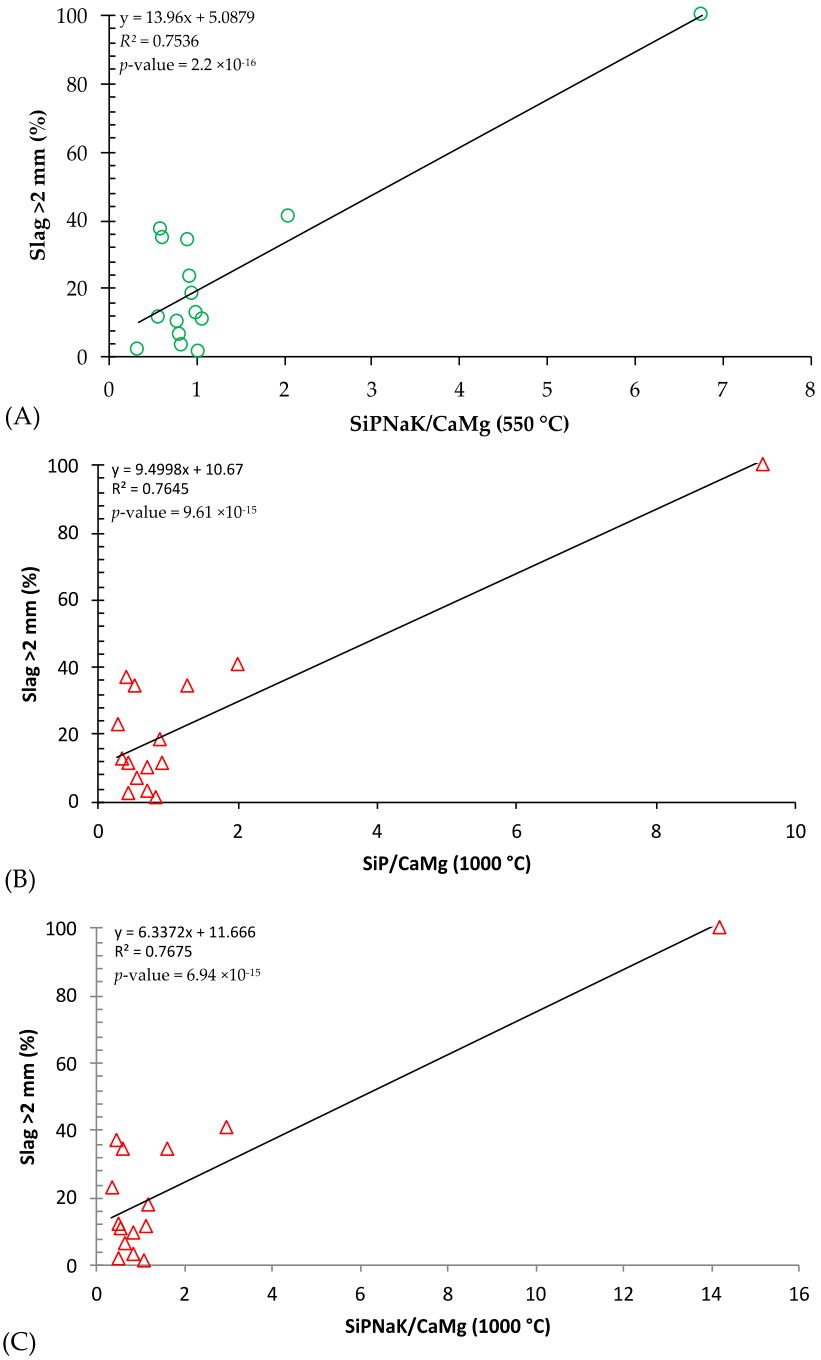

Figure 8. Correlations of the accumulated percentage of slag >2.00 mm measured in the BioSlag test. Graphs shown the equation and R^2 values: (**A**) Percentage of slags and SiP/CaMg index at 550 °C; (**B**,**C**) Percentage of slags and SiPNaK/CaMg index at 550 and 1000 °C, respectively.

Pellets from the different types of biomasses subjected to the BioSlag test showed significant differences ($p \leq 0.05$) according to the Kruskal–Wallis test. The pellets from Penn showed great formation of slags since their ashes presented high fusibility problems (Figure 9 in red color). On the other hand, the pellets from Jun, Pipa, Queco, Quela, Cari and Pidu pellets were the ones that presented the fewest problems (Severity index < 0.2).

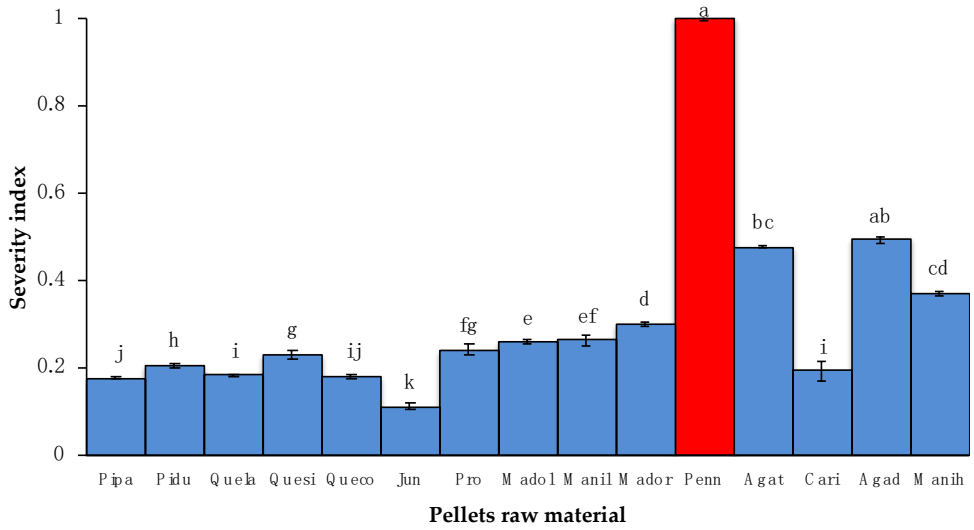

Figure 9. Severity index calculated based on the BioSlag test. The lines above the bars show the standard deviation, species with different letters are statistically different ($p < 0.05$). The bar in red color corresponds to biomass pellets with high fusibility problems.

3.3. Percentage of Calcined Sample

The percentage of calcined samples of pellets from different sources presented statistically significant differences ($p \leq 0.05$); the percentage of calcined samples of pellets from forest origin Pipa, Pidu, Quela, Quesi, Queco, Jun and Pro varied between 0.36% and 1.54%; the percentage of calcined samples of pellets from agricultural origin Madol, Manil, Mador and Penn ranged between 1.41 and 7.43%, and the highest percentage value was presented by Penn (*Pennisetum* sp.). Finally, the percentage of pellets from agro-industrial origin Agat, Cari, Agad and Manih ranged from 1.53 to 8.81% and was the origin with the highest amount of slag (Figure 10).

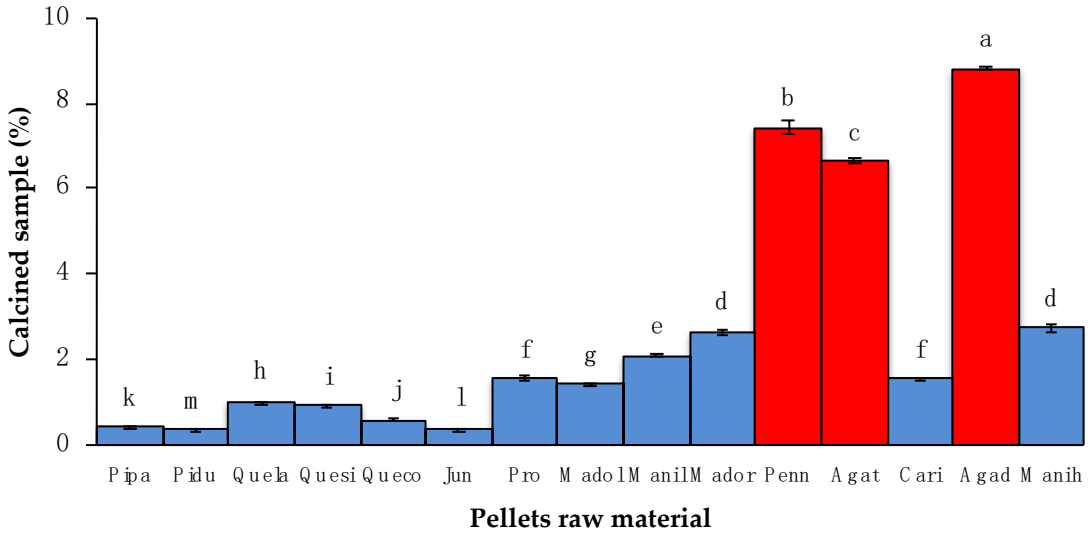

Figure 10. Percentage of calcined sample of the BioSlag test. The lines above the bars show the standard deviation, the species with different letters are statistically different ($p < 0.05$). The bars in red color correspond to biomass pellets with high fusibility problems.

4. Discussion

4.1. Chemical Elements Composition of Pellet Ashes from Different Sources

The concentration of the alkaline earth metals CaO and MgO in the ashes of the pellets was slightly reduced when subjected to calcination processes at 550 and 1000 °C because

they are refractory elements and remain solid at high combustion temperatures. La Puerta et al. [37] found similar results in CaO (31.79%) and MgO (8.17%) concentrations on *Pinus pinaster* pruning, while Moilanen [38] reported values for pine sawdust of CaO (41.8%) and MgO (11.8%) and for pine bark of 40.6 and 4.5%, respectively. These last data are very similar to those obtained for Pipa and Pidu pellets. Some authors registered concentrations up to 36.5% for CaO and 9.22% for MgO from oak shavings [25]. Contents of CaO (45.56%) and MgO (7.48%) have been found in forest residues, although values of 35.7 and 4.4% have also been reported on the same material type [39]. Except for Penn and Manih pellets, agricultural and agro-industrial pellets had CaO contents greater than 30%, and the MgO contents were greater than 4%. This contrasts with some authors who report very low values of CaO for herbaceous plants. For example, in bamboo plants, CaO values of 4.46% were reported, and in banana grass (*Pennnisetum* sp.) the value was 4.09%. These values are very similar to the Penn sample analyzed at 1000 °C (4.49%) as well as to Arundo grass, with values of 2.98% and 5.41%. In addition, there are reports of 3.31% in reed canary grass [38,40]. High CaO contents in biomass have been associated with bark residues. High concentrations of CaO and MgO can counteract low melting points, caused most often by the contents of K and Na, so it is recommended to add limestone, dolomite or periclassic to fuels made from straw or herbaceous plants as a way to control slag formation, agglomeration and SO_2 emissions.

The K_2O content in the pellet ash from all sources shows a considerable reduction from 550 °C to 1000 °C, agreeing with previous observations for K volatilization. Different behavior was shown by the Na_2O concentrations. However, this element did not change between both temperatures because alkali metals such as K_2O are the least stable oxides that make up the ashes, so at combustion temperatures above 550 °C they can be reduced in the form of metal vapor or could even react with water vapor to form stable and relatively volatile hydroxides (KOH and NaOH). On the other hand, it was observed that K loss from 550 °C to 1000 °C, caused by volatilization, is greater in fuels with low silica contents, supporting previous observations [41]. The K_2O contents at 550 °C were higher in the ashes of pellets from forest origin, as shown for Quela (21.29%), Pro (29.75%) and Queco (29.95%). Regarding to the percentage of K_2O in ashes produced at 1000 °C, the values were relatively low for Quela (4.87%), Pipa (6.97%) and Quesi (7.46%). Similar values were reported in wood samples with K_2O contents of 16.78% and 0.77% for Na_2O, while in the pruning of pines, K_2O concentration was 22.32%, with 0.42% for NaO_2. For agricultural samples, such as olive wood, the values were 24.7% and 3.4%, respectively, and for vine shoots the values were 22.3 and 5.4% for K_2O and Na_2O, respectively [37,41]. As can be seen, biomass of herbaceous origin was the most problematic when used in combustion due to its high K_2O content; concentrations of 49.08% have been found in banana grass, 53.38% in bamboo and 56.69% in Cynara stems, and a very similar value was obtained for Penn samples, which are ashes of *Pennisetum* sp. pellets [40]. Pellets with high concentrations of K and with relatively high amounts of silica and low amounts of Ca and Mg can react with the Si dispersed in the organic structure of the biofuel and form an alkaline-sticky silicate melt that is the principle for the formation of slags [28].

The highest SiO_2 content at 550 °C was in the pellet ashes from Pipa (28.24%), Penn (27.32%) and Agad (23.68%), followed by Pidu and Quesi with 22.49 and 21.10% respectively, while for ashes generated at 1000 °C, the highest concentrations were in Penn (56.75%), Agad (38.34%), Quesi (30.65%), Cari (30.03%) and Manil (29.84%). Therefore, it is shown that the content of SiO_2 increases when increasing the combustion temperature, mainly in samples of agricultural and agro-industrial origin. Similar results have been obtained by burning *Miscanthus giganteus* grass (54.4%), wheat straw (64.3%) and spruce wood (49.5%) at temperatures above 900 °C [42]. Viana et al. [43] found high concentrations of this element in the woody biomass of shrubs *Ulex europaeu* (33.6%), *Cytisus multiflorus* (16.6%) and *Erica australis* (17.0%). In general terms, wood free of contamination contains very limited amounts of Si, so it does not represent high risk of the formation of sticky silicates in heaters that work above 1000 °C; the opposite happens with contaminated

wood since this favors the formation of sticky silicates and slag problems [44]. Pellets with high concentrations of Si and alkali metals tend to form slags, such as pellets made from herbaceous materials or straw [45].

Concentrations of metalloids such as Fe_2O_3 were relatively low at 550 °C; the highest content was presented in the ashes from Pipa (4.17%), Jun (3.40%) and Pidu (3.30%), while for MnO, the greatest values were in Pidu (3.33%), Quesi (1.76%) and Queco (1.53%). In Fe_2O_3 at 1000 °C, concentration for Quesi was 4.75%, for Pidu was 4.17% and for Jun was 4.12%, and for MnO in Pidu pellets, it was 4.49%, for Queco it was 2.89% and for Cari it was 1.77%. There are reports of Fe_2O_3 contents similar to those obtained in the present work in pellets from walnut husk (2.4%), red oak wood (9.5%), wheat straw (3.5%) and hazelnut husk (3.1%) [46]. The pollutants in residues and/or additives in biofuels increase the agglomeration of metalloids in combustion equipment [47].

Finally, the highest concentrations of Al_2O_3 at 550 °C were registered in Pipa pellets (3.69%), Agat (2.21%) and Pidu (2.13%). The content of P_2O_5 on Manil was 3.71%, for Manih was 2.97% and for Quela was 2.14%. At 1000 °C, the content of Al_2O_3 was 10.75% in Pipa, 6.60% in Pidu and 6.59% in Quesi. The P_2O_5 concentration for pellets from Quela was 19.94%, for Manih was 19.75% and for Manil was 18.78%. There are reports of The Al_2O_3 concentration for biomass for forest residues was 3.55%, for almond shell was 2.7%, for red oak wood was 9.5%, for walnut husk was 2.4% and for wheat straw was 3.5%. The P_2O_5 contents were 0.44%, 4.5%, 1.8%, 6.2% and 3.5%, respectively [11,48]. During combustion processes, Al forms alumina (Al_2O_3), which is a solid compound that does not participate significantly in the chemistry of ash [49]. It has been found in wood pellets and chips where high concentrations of P form low melting point phosphate salts, which cause the formation of partially molten ash particles that aggravate agglomeration, slag formation and fouling of boilers [50]. During combustion, K-rich phosphates have very low melting points ranging from 650 to 700 °C [51], which is why phosphate-rich ash reacts by forming layers of silicate/phosphate coatings that are responsible for the agglomeration process. During this process, potassium reacts with the Si present in the organic structure and/or mineral surfaces of the biofuel, the melt of sticky silicate is formed locally on these surfaces, and other ash-forming elements such as calcium and magnesium, which are frequently found in wood-derived fuels, could then dissolve in the melt [45]. However, the problems related to P for ash continue to be a confusing process and further studies are required.

The relationship among chemical components in ashes was explained by PCA, which allows the reduction of sets of variables, and in addition to that, it can explain up to 88% of the elements variation and create groups in principal components CP to facilitate the interpretation of the studied data [52]. The PCA grouped samples with similar ash element concentrations at 550 °C. The elements CaO and Na_2O were grouped with the pellets from Agat, Car, Agad and Jun; K_2O and P_2O_5 were grouped with the pellets from Penn, Manih and Queco; and the concentrations of Al_2O_3, Fe_2O_3, SiO_2, MnO and MgO were grouped with the pellets from Quesi, Pidu and Pipa. The samples of Madol, Manil, Mador, Quela and Pro were not associated with any element in the CP. At 1000 °C, the concentrations of CaO, Na_2O, P_2O_5 and MgO were grouped with the pellets from Madol, Queco, Quela and Pro; Al_2O_3, Fe_2O_3 and MnO were grouped with the pellets from Pipa, Pidu, Quesi and Jun; the elements SiO_2 and K_2O were grouped with the pellets from Cari, Agad and Penn; and finally, the pellets from Manih, Mador and Manil were not associated with any element in the CP. Therefore, if any of these groups were burned together, they would present similar results.

4.2. Slag Prediction Indexes of Ash from 15 Sources of Pelletized Biomass

Melting at 1000 °C was observed for agricultural pellets (Penn), with the highest values of K_2O (56% at 550 °C) and NaK/B index (0.82), together with the highest values of SiP/CaMg and SiPNaK/CaMg (2.28 and 6.77). This supports previous observations in some herbaceous biofuels (rice straw, wheat straw, corn straw) that the behavior of ash melting is influenced by the alkali/alkaline earth ratio and that the chemical composition

of these pellets can reach very high values of K and very low values of Ca. [53] The level of SiO_2 in Penn samples was above the threshold of >25 % proposed for this element by Toscano et al. [33], supporting that high silica contents in low P fuels can be an indicator of slagging risk [40], particularly when accompanied by alkali metals. This also supports observations using chemical equilibrium model calculations by Öhman et al. [45], who suggested increased formation of "sticky" silicate melt (i.e., increased slagging tendency) when higher SiO_2 contents were added to the fuel ash composition at typical burner operating conditions. The Mani sample, with the second highest K_2O (42% at 550 °C) and high NaK/B, also presented significant slagging problems, with 28.3% of slag > 3.15, but lower than Penn, which might be explained by a relatively lower SiO_2 content (18%). Furthermore, samples with similar levels of Si to Penn, but with lower K levels, showed a less problematic behavior, supporting the notion that the presence of both elements, Si and K, might be required for significant ash melting and slagging to occur. This would agree with the observations of Gilbe et al. [28], who found that, according to the calculated chemical/physical slag formation processes, potassium containing biomass fuels relatively rich in silicon (either dispersed in the organic structure or contaminated with sand) with relatively low amounts of alkaline earth metals (Ca, Mg) retain a part of the potassium, forming a sticky alkali-silicate melt which is a prerequisite for the slag formation process.

In this sense, the indexes based on SiP/CaMg and SiPNaK/CaMg best explained the measured value of slags in the BioSlag test by sieve of 2.00 mm, with a value of $R^2 > 0.75$ obtained for the prediction of pellet slags. These results support the good predictability ($R^2 > 0.7$) of those indexes for slag formation [31].

In addition to capturing full ash melting, the BioSlag test also captured moderate levels of slagging for a variety of pellets, supporting the previously observed sensitivity of this test for capturing varying degrees of ash slagging [20,39] for a further variety of woody and agricultural fuels. Future studies could analyze the use of biomass mixtures or include additives to minimize the slagging tendency, validated both with both laboratory BioSlag tests and combustion experiments in operational boilers.

4.3. Percentage of Calcined Sample of Pellets

The percentage of calcined samples of pellets from 15 biomass origins was highly variable, with pellets from forest origin presenting lower values (0.35–1.54%). Correa-Méndez et al. [54], when studying and evaluating the physicochemical characteristics of sawdust and shavings of *Pinus leiophylla*, *P. montezumae* and *P. pseudostrobus*, also reported low ash content values (0.26 ± 0.3% and 0.34 ± 0.30%, respectively), similar to those in pellets made from wheat straw mixtures that have very high ash contents (11.43–13.06%) [55]. In the present work, it was found that pellets from Agat, Penn and Agad had values of 6.64, 7.43 and 8.81%, respectively. Pellets from forest origin with low percentages of calcined samples meet the standards for manufacturing pellets and briquettes because they have low ash contents, and a strong relationship was found between ash content and slag formation. Similarly, high contents of Ca and Mg increase the melting point of ash, and additionally point out that a high ash content can affect combustion equipment and residential users by increasing cleaning processes [54]. Some pellets have highly varied ash contents, as was reported for poplar wood (2.2%) and grass (8.5%); the latter generates more ash due to its high content of K_2O [56].

5. Conclusions

The behavior of pellets made from biomass in different combustion processes is of great importance and applicability, and the formation of slag is associated with the chemical composition of the material and the temperature at which it is combusted.

Biomass recommended for producing pellets for their low risks of slag formation are from forest origin, such as *Pinus patula*, *P. durangensis*, *Quercus laeta*, *Q. sideroxyla*, *Q. conzattii*, *Juniperus* sp. and *Prosopis* sp., while pellets from agro-industrial sources (*Pennisetum* sp., *Agave durangensis*, *Agave tequilana* and *Mangifera indica* bone) showed a high risk of slag

formation at 550 and 1000 °C. The chemical composition of biomass sources affects the level of sintering and slag formation. Pellets from biomass origins with low or moderate CaO values and very high amounts of K_2O and P_2O_5 have high risks of sintering, while combustion at low temperatures can greatly reduce the formation of slags. On the other hand, the indexes NaK/B, SiP/CaMg, and SiPNaK/CaMg were effective for the prediction of slag formation risks, as measured by the BioSlag test.

Supplementary Materials: The following supporting information can be downloaded at: https://www.mdpi.com/article/10.3390/en15145026/s1. Data used to elaborate some graphics were added to Annexes S1–S4.

Author Contributions: Conceptualization, A.C.-P., J.C.C.-T. and M.N.H.; methodology, A.C.-P. and D.J.V.-N.; validation, D.J.V.-N., J.A.P.-R. and C.A.N.-B.; formal analysis, A.C.-P., J.C.C.-T., D.J.V.-N. and J.A.P.-R.; investigation, J.C.C.-T. and C.A.N.-B.; resources, A.C.-P., D.J.V.-N., M.N.H. and J.A.P.-R.; writing—original draft preparation, J.C.C.-T. and A.C.-P.; writing—review and editing, M.N.H. and J.A.P.-R.; visualization, C.A.N.-B.; funding acquisition, A.C.-P. All authors have read and agreed to the published version of the manuscript.

Funding: This research was funded by SENER-CONACYT "Fondo de Sustentabilidad Energética", grant number SENER-CONACYT 2014 246911 "Clúster de Biocombustibles Sólidos para la generación térmica y eléctrica" and CONACYT project 166444.

Data Availability Statement: No applicable.

Acknowledgments: The publication of this article was funded by the authors and by Consejo de Ciencia y Tecnología del Estado de Durango (COCYTED).

Conflicts of Interest: The authors declare no conflict of interest.

References

1. Martinopoulos, G.; Papakostas, K.T.; Papadopoulos, A.M. A comparative review of heating systems in EU countries, based on efficiency and fuel cost. *Renew. Sustain. Energy Rev.* **2018**, *90*, 687–699. [CrossRef]
2. Thomson, H.; Liddell, C. The suitability of wood pellet heating for domestic households: A review of literature. *Renew. Sustain. Energy Rev.* **2015**, *42*, 1362–1369. [CrossRef]
3. Wöhler, M.; Andersen, J.S.; Becker, G.; Persson, H.; Reichert, G.; Schön, C.; Schmidl, C.; Jaeger, D.; Pelz, S.K. Investigation of real life operation of biomass room heating appliances—Results of a European survey. *Appl. Energy* **2016**, *169*, 240–249. [CrossRef]
4. Rodríguez, J.L.; Álvarez, X.; Valero, E.; Ortiz, L.; de la Torre-Rodríguez, N.; Acuña-Alonso, C. Influence of ashes in the use of forest biomass as source of energy. *Fuel* **2021**, *283*, 119256. [CrossRef]
5. Arifianti, Q.A.M.O.; Rahmat, A.; Anggarini, U.; Nugrahani, E.F.; Ummatin, K.K. Production of Briquettes to Utilize Woody Cutting Waste at Universitas Internasional Semen Indonesia (UISI). *J. Phys. Conf. Ser.* **2021**, *1803*, 12012. [CrossRef]
6. Kanageswari, S.V.; Tabil, L.G.; Sokhansanj, S. Dust and Particulate Matter Generated during Handling and Pelletization of Herbaceous Biomass: A Review. *Energies* **2022**, *15*, 2634. [CrossRef]
7. Royo, J.; Canalís, P.; Zapata, S.; Gómez, M.; Bartolomé, C. Ash Behaviour during Combustion of Agropellets Produced by an Agro-Industry—Part 2: Chemical Characterization of Sintering and Deposition. *Energies* **2022**, *15*, 1499. [CrossRef]
8. Acda, M.N.; Devera, E.E. Physico-chemical properties of wood pellets from forest residues. *J. Trop. For. Sci.* **2014**, *26*, 589–595.
9. Barbanera, M.; Lascaro, E.; Stanzione, V.; Esposito, A.; Altieri, R.; Bufacchi, M. Characterization of pellets from mixing olive pomace and olive tree pruning. *Renew. Energy* **2016**, *88*, 185–191. [CrossRef]
10. Carrillo-Parra, A.; Contreras-Trejo, J.C.; Pompa-García, M.; Pulgarín-Gámiz, M.A.; Rutiaga-Quiñones, J.G.; Pámanes-Carrasco, G.; Ngangyo-Heya, M. Agro-pellets from oil palm residues/pine sawdust mixtures: Relationships of their physical, mechanical and energetic properties, with the raw material chemical structure. *Appl. Sci.* **2020**, *10*, 6383. [CrossRef]
11. Fernández Llorente, M.J.; Escalada Cuadrado, R.; Murillo Laplaza, J.M.; Carrasco García, J.E. Combustion in bubbling fluidised bed with bed material of limestone to reduce the biomass ash agglomeration and sintering. *Fuel* **2006**, *85*, 2081–2092. [CrossRef]
12. Kleinhans, U.; Wieland, C.; Frandsen, F.J.; Spliethoff, H. Ash formation and deposition in coal and biomass fired combustion systems: Progress and challenges in the field of ash particle sticking and rebound behavior. *Prog. Energy Combust. Sci.* **2018**, *68*, 65–168. [CrossRef]
13. Frandsen, F.J. Utilizing biomass and waste for power production—A decade of contributing to the understanding, interpretation and analysis of deposits and corrosion products. *Fuel* **2005**, *84*, 1277–1294. [CrossRef]
14. Szemmelveisz, K.; Szucs, I.; Palotás, Á.B.; Winkler, L.; Eddings, E.G. Examination of the combustion conditions of herbaceous biomass. *Fuel Process. Technol.* **2009**, *90*, 839–847. [CrossRef]

15. Thyrel, M.; Samuelsson, R.; Finell, M.; Lestander, T.A. Critical ash elements in biorefinery feedstock determined by X-ray spectroscopy. *Appl. Energy* **2013**, *102*, 1288–1294. [CrossRef]
16. Chen, C.; Bi, Y.; Huang, Y.; Huang, H. Review on slagging evaluation methods of biomass fuel combustion. *J. Anal. Appl. Pyrolysis* **2021**, *155*, 105082. [CrossRef]
17. Vassilev, S.V.; Vassileva, C.G.; Song, Y.-C.; Li, W.-Y.; Feng, J. Ash contents and ash-forming elements of biomass and their significance for solid biofuel combustion. *Fuel* **2017**, *208*, 377–409. [CrossRef]
18. Shao, Y.; Wang, J.; Preto, F.; Zhu, J.; Xu, C. Ash deposition in biomass combustion or co-firing for power/heat generation. *Energies* **2012**, *5*, 5171–5189. [CrossRef]
19. Vassilev, S.V.; Baxter, D.; Andersen, L.K.; Vassileva, C.G. An overview of the composition and application of biomass ash.: Part 2. Potential utilisation, technological and ecological advantages and challenges. *Fuel* **2013**, *105*, 19–39. [CrossRef]
20. Melissari, B. Comportamiento de Cenizas y su Impacto en Sistemas de Combustión de Biomasa. *Mem. Trab. Difus. Cient. Téc.* **2012**, *10*, 69–82.
21. Du, S.; Yang, H.; Qian, K.; Wang, X.; Chen, H. Fusion and transformation properties of the inorganic components in biomass ash. *Fuel* **2014**, *117*, 1281–1287. [CrossRef]
22. Mlonka-Mędrala, A.; Magdziarz, A.; Gajek, M.; Nowińska, K.; Nowak, W. Alkali metals association in biomass and their impact on ash melting behaviour. *Fuel* **2020**, *261*, 116421. [CrossRef]
23. Llorente, M.J.F.; García, J.E.C. Comparing methods for predicting the sintering of biomass ash in combustion. *Fuel* **2005**, *84*, 1893–1900. [CrossRef]
24. Miles, T.R.; Miles, T.R.; Baxter, L.L.; Bryers, R.W.; Jenkins, B.M.; Oden, L.L. Boiler deposits from firing biomass fuels. *Biomass Bioenergy* **1996**, *10*, 125–138. [CrossRef]
25. Vega-Nieva, D.J.; Ortiz Torres, L.; Míguez Tabares, J.L.; Morán, J. Measuring and Predicting the Slagging of Woody and Herbaceous Mediterranean Biomass Fuels on a Domestic Pellet Boiler. *Energy Fuels* **2016**, *30*, 1085–1095. [CrossRef]
26. Feldmeier, S.; Wopienka, E.; Schwarz, M.; Schön, C.; Pfeifer, C. Applicability of Fuel Indexes for Small-Scale Biomass Combustion Technologies, Part 1: Slag Formation. *Energy Fuels* **2019**, *33*, 10969–10977. [CrossRef]
27. Jablonowski, N.D.; Kollmann, T.; Nabel, M.; Damm, T.; Klose, H.; Müller, M.; Bläsing, M.; Seebold, S.; Krafft, S.; Kuperjans, I. Valorization of Sida (Sida hermaphrodita) biomass for multiple energy purposes. *GCB Bioenergy* **2017**, *9*, 202–214. [CrossRef]
28. Gilbe, C.; Marcus, O.; Lindstro, E.; Bostro, D.; Backman, R.; Samuelsson, R.; Burvall, J. Slagging Characteristics during Residential Combustion of Biomass Pellets. *Energy Fuels* **2008**, *22*, 3536–3543. [CrossRef]
29. Hansen, H.; Jensen, T. Measuring solid biofuels' slag tendencies during combustion. In Proceedings of the 16th European Biomass Conference & Exhibition, Valencia, Spain, 2–6 June 2008.
30. Rathbauer, J.; Schön, C.; Vega-Nieva, D.; Hartmann, H.; Ortiz, L. Simplified method for slag prediction–PASSA method. In Proceedings of the Pellets Conference, Berlin, Germany, 26–27 February 2014.
31. Schön, C.; Feldmeier, S.; Hartmann, H.; Schwabl, M.; Dahl, J.; Rathbauer, J.; Vega-Nieva, D.J.; Boman, C.; Öhman, M.; Burval, J. New Experimental Evaluation Strategies Regarding Slag Prediction of Solid Biofuels in Pellet Boilers. *Energy Fuels* **2019**, *33*, 11985–11995. [CrossRef]
32. Mack, R.; Kuptz, D.; Schön, C.; Hartmann, H. Combustion behavior and slagging tendencies of kaolin additivated agricultural pellets and of wood-straw pellet blends in a small-scale boiler. *Biomass Bioenergy* **2019**, *125*, 50–62. [CrossRef]
33. Toscano, G.; Feliciangeli, G.; Rossini, G.; Fabrizi, S.; Pedretti, E.F.; Duca, D. Engineered solid biofuel from herbaceous biomass mixed with inorganic additives. *Fuel* **2019**, *256*, 115895. [CrossRef]
34. Carrillo-Parra, A.; Rutiaga-Quiñones, J.G.; Ríos-Saucedo, J.C.; Ruiz-García, V.M.; Ngangyo-Heya, M.; Nava-Berumen, C.A.; Núñez-Retana, V.D. Quality of Pellet Made from Agricultural and Forestry Waste in Mexico. *BioEnergy Res.* **2021**, *15*, 977–986. [CrossRef]
35. *UNE-EN ISO 18122*; Biocombustibles Sólidos. Método para la Determinación del Contenido en Cenizas. UNE: Genova, Spain, 2016.
36. Rodrigues, A.; Nunes, L.J.R. Evaluation of ash composition and deposition tendencies of biomasses and torrefied products from woody and shrubby feedstocks: SRC poplar clones and common broom. *Fuel* **2020**, *269*, 117454. [CrossRef]
37. Lapuerta, M.; Hernández, J.J.; Pazo, A.; López, J. Gasification and co-gasification of biomass wastes: Effect of the biomass origin and the gasifier operating conditions. *Fuel Process. Technol.* **2008**, *89*, 828–837. [CrossRef]
38. Moilanen, A. *Thermogravimetric Characterisations of Biomass and Waste for Gasification Processes*; VTT Technical Research Centre of Finland: Espoo, Finland, 2006; Volume 60.
39. Blomquist, J.; Skrifvars, B.; Backman, R.; Hupa, M. The prediction of behaviour of ashes from five different solid fuels in fluidised bed combustion. *Fuel Energy Abstr.* **2001**, *42*, 24–25. [CrossRef]
40. Scurlock, J.M.O.; Dayton, D.C.; Hames, B. Bamboo: An overlooked biomass resource? *Biomass Bioenergy* **2000**, *19*, 229–244. [CrossRef]
41. Thy, P.; Grundvig, S.; Jenkins, B.M.; Shiraki, R.; Lesher, C.E. Analytical controlled losses of potassium from straw ashes. *Energy Fuels* **2005**, *19*, 2571–2575. [CrossRef]
42. Holubcik, M.; Jandacka, J. Chemical composition in relation with biomass ash structure. *AIP Conf. Proc.* **2014**, *1608*, 42–47. [CrossRef]

43. Viana, H.; Vega-Nieva, D.J.; Ortiz Torres, L.; Lousada, J.; Aranha, J. Fuel characterization and biomass combustion properties of selected native woody shrub species from central Portugal and NW Spain. *Fuel* **2012**, *102*, 737–745. [CrossRef]
44. Nordin, A. Chemical elemental characteristics of biomass fuels. *Biomass Bioenergy* **1994**, *6*, 339–347. [CrossRef]
45. Öhman, M.; Nordin, A.; Hedman, H.; Jirjis, R. Reasons for slagging during stemwood pellet combustion and some measures for prevention. *Biomass Bioenergy* **2004**, *27*, 597–605. [CrossRef]
46. Demirbas, A. Combustion characteristics of different biomass fuels. *Prog. Energy Combust. Sci.* **2004**, *30*, 219–230. [CrossRef]
47. Yan, J.; Karlsson, A.; Zou, Z.; Dai, D.; Edlund, U. Contamination of heavy metals and metalloids in biomass and waste fuels: Comparative characterisation and trend estimation. *Sci. Total Environ.* **2019**, *19*, 134382. [CrossRef]
48. Demirbaş, A. Sustainable cofiring of biomass with coal. *Energy Convers. Manag.* **2003**, *44*, 1465–1479. [CrossRef]
49. Zevenhoven, M.; Yrjas, P.; Skrifvars, B.J.; Hupa, M. Characterization of ash-forming matter in various solid fuels by selective leaching and its implications for fluidized-bed combustion. *Energy Fuels* **2012**, *26*, 6366–6386. [CrossRef]
50. Piotrowska, P.; Zevenhoven, M.; Hupa, M.; Davidsson, K.; Amand, L.E.; Zabetta, E.C.; Barišić, V. Fate of Phosphorus during Co-Combustion of Rapseed Cake with Wood. In Proceedings of the 20th International Conference on Fluidized Bed Combustion, Xi'an, China, 18–21 May 2009; pp. 979–986. [CrossRef]
51. Lindström, E.; Sandström, M.; Boström, D.; Öhman, M. Slagging characteristics during combustion of cereal grains rich in phosphorus. *Energy Fuels* **2007**, *21*, 710–717. [CrossRef]
52. Szczepanik, M.; Szyszlak-Bargłowicz, J.; Zając, G.; Koniuszy, A.; Hawrot-Paw, M.; Wolak, A. The Use of Multivariate Data Analysis (HCA and PCA) to Characterize Ashes from Biomass Combustion. *Energies* **2021**, *14*, 6887. [CrossRef]
53. Yao, X.; Zhao, Z.; Li, J.; Zhang, B.; Zhou, H.; Xu, K. Experimental investigation of physicochemical and slagging characteristics of inorganic constituents in ash residues from gasification of different herbaceous biomass. *Energy* **2020**, *198*, 117367. [CrossRef]
54. Correa-Méndez, F.; Carrillo-Parra, A.; Rutiaga-Quiñones, J.G.; Márquez-Montesino, F.; González-Rodríguez, H.; Jurado-Ybarra, E.; Garza-Ocañas, F. Contenido de humedad y sustancias inorgánicas en subproductos maderables de pino para su uso en pélets y briquetas. *Rev. Chapingo Ser. Cienc. For. Ambient.* **2014**, *20*, 77–88. [CrossRef]
55. Ríos-Badrán, I.M.; Luzardo-Ocampo, I.; García-Trejo, J.F.; Santos-Cruz, J.; Gutiérrez-Antonio, C. Production and characterization of fuel pellets from rice husk and wheat straw. *Renew. Energy* **2020**, *145*, 500–507. [CrossRef]
56. Hedayati, A.; Lindgren, R.; Skoglund, N.; Boman, C.; Kienzl, N.; Öhman, M. Ash Transformation during Single-Pellet Combustion of Agricultural Biomass with a Focus on Potassium and Phosphorus. *Energy Fuels* **2021**, *35*, 1449–1464. [CrossRef]